

Density of states and dc electrical conductivity in an order-disorder ternary alloy in a generalized coherent-potential approximation

William Karstens and Leonard M. Scarfone

Department of Physics, University of Vermont, Burlington, Vermont 05405

(Received 26 November 1990)

By using a generalized version of the coherent-potential approximation, we investigate the effect of long-range order on the electronic properties of a model ternary alloy. Previous considerations by Plischke and Mattis of a second-order phase transition in a three-dimensional order-disorder binary alloy necessitated the introduction of a bipartite lattice in which each atom occupies its own sublattice in perfect order. The present case, in particular, contains the influence of a completely random third atom on the density of states and the dc electrical conductivity of the binary system. Numerical results, in the form of plots of these properties for representative values of the scattering strengths and the atomic concentrations, over the range of the order parameter, are presented. Calculation of the temperature dependence of the order parameter shows that at and above the critical temperature, as this parameter approaches zero, the model reduces to the disordered ternary alloy. For comparison, it is shown that this behavior also follows from the traditional order-disorder transition picture of the Bragg-Williams approximation.

I. INTRODUCTION

The subject of the electronic properties of disordered alloys has received extensive, if not exhaustive study over the past several decades. This is due in large part to the success of the coherent-potential approximation (CPA) introduced by Soven¹ and others.² Subsequently, several advanced techniques have been combined with the CPA. One of the more ambitious of these approaches is the Korringa-Kohn-Rostoker coherent-potential approximation (KKR-CPA).³ Examples of this method may be found in the works of Butler, Stocks, and Winter.^{4,5} More recently, many-body theory has been incorporated with the CPA by Vignale *et al.*⁶ and Joubert and Inkson.⁷ Clearly, these methods significantly raise the complexity (both analytically and computationally) of the order-disorder problem to be considered here and thus will not be considered further. Not long after the introduction of the CPA did efforts turn toward the use of this band-model picture of a description of long-range ordering in binary alloys. This was first done in one dimension by Foo and Amar⁸ and later by Plischke and Mattis,⁹ who calculated the density of states (DOS) for a three-dimensional binary alloy with a second-order phase transition. Within the same context, the dc electrical conductivity was investigated by Paja,¹⁰ Borodachev *et al.*,¹¹ and Kudrnovský and Velický.¹²

The DOS and the dc conductivity of a disordered ternary alloy have been calculated, respectively, by Scarfone¹³ and Wysokinski and Pilat.¹⁴ Similar work is performed here for a ternary alloy which may be thought of as an order-disorder binary alloy with a completely random third atom on a bipartite lattice.¹⁵ Section II briefly reviews the traditional order-disorder transition picture of the quasicheical Bragg-Williams approximation¹⁶ in the framework of the ternary system. The temperature

dependence of the long-range order (LRO) parameter is obtained in a form identical to the binary result of Brouers *et al.*¹⁷ As expected, a second-order phase transition from the ordered to the disordered binary state occurs. However, an element of disorder persists in the system since the third atom is random over both sublattices at all stages of ordering. Section III introduces the CPA in the generalized description of the bipartite lattice. This requires the use of two coherent potentials and leads to a pair of coupled, nonlinear complex equations for their determination. The solutions to these equations constitute the bulk of the numerical analysis. Section IV is concerned with the band-model calculation of the temperature dependence of the LRO parameter through the use of moments of the DOS for the ternary alloy. The results coincide with those obtained in the Bragg-Williams approach, thus providing satisfactory contact between these two mean-field theories. Section V deals with the CPA electrical conductivity problem within the order-disorder framework. The expression for this quantity is seen to reduce to two integrals which can be evaluated in closed form in the complex energy plane. Section VI presents numerical examples and discussion of the DOS and the dc conductivity for the ternary alloy. Although a wide range of values of the input data are possible, we select only those permitting a convenient comparison with results in the literature. Finally, concluding remarks are given in Sec. VII.

II. BRAGG-WILLIAMS APPROXIMATION AND THE ORDER-DISORDER PHASE TRANSITION IN THE TERNARY ALLOY

As a way of establishing the relevant concepts and variables, as well as providing a general picture of the ternary alloy thermodynamics, we briefly review the order-

disorder problem in the context of the Bragg-Williams approximation. We first imagine a simple cubic lattice, with N sites, divided into two equal sublattices labeled by α and β . The number of sites on each sublattice is

$$N_\alpha = N_\beta = \frac{1}{2}N. \quad (2.1)$$

We assume a structure such that each $\alpha(\beta)$ site has only $\beta(\alpha)$ sites as nearest neighbors, thus creating a CsCl-type lattice. For the ternary alloy, three types of atoms are distributed over these sites such that

$$N_A + N_B + N_C = N, \quad (2.2)$$

where N_A , N_B , and N_C are the numbers of A , B , and C atoms, respectively. Their fractional concentrations are then given by

$$X_A = \frac{N_A}{N}, \quad X_B = \frac{N_B}{N}, \quad X_C = \frac{N_C}{N}. \quad (2.3)$$

In general, a complete ordering of all three atoms requires the use of three sublattices. Since we have only two sublattices it should be clear that we are considering a restricted form of ordering. In particular, while the A and B atoms participate in the ordering process the C atom will always remain completely random. Thus, we may imagine our system as an order-disorder binary alloy with a random third atom. To this end we define a LRO parameter, η , in the following way. For $X_A \leq X_B$,

$$\eta = \frac{N_A^\alpha - N_A^\beta}{N_A^\alpha + N_A^\beta} = \frac{P_A^\alpha - P_A^\beta}{P_A^\alpha + P_A^\beta}, \quad (2.4)$$

where, for example, N_A^β and P_A^β represent the number and probability of an A atom occurring on the β lattice. The former are defined by $N_n^\sigma = N^\sigma P_n^\sigma$ for $\sigma \in \{\alpha, \beta\}$ and $n \in \{A, B, C\}$, while the latter are explicitly given by

$$\begin{aligned} P_A^\alpha &= X_A + X_A \eta, & P_B^\alpha &= X_B - X_A \eta, \\ P_A^\beta &= X_A - X_A \eta, & P_B^\beta &= X_B + X_A \eta. \end{aligned} \quad (2.5)$$

Since the C atom is random, we also have $P_C^\alpha = P_C^\beta = X_C$. To obtain results for $X_A \geq X_B$ simply replace A with B and exchange α with β in the LRO parameter definition, and let $X_A \rightarrow X_B$ in the η coefficients in the above probability factors. Notice that, for $\eta=0$, these probabilities reduce to the ordinary fractional concentrations while for $\eta=1$, the P_n^σ put all of the A atoms on the α lattice and all of the B atoms on the β lattice (for equal concentrations of A and B atoms). For unequal concentrations, the factors describe the excess of one ordering atom on the other lattice.

The first step in providing a quantitative picture of the thermodynamics is to construct the configurational energy associated with the interaction between nearest-neighbor pairs. We write this as

$$E = - \sum_{m,n} \mathcal{E}_{mn} N_{mn}, \quad (2.6)$$

where the N_{mn} are the number of m - n pairs (counting N_{AB} and N_{BA} only once), and \mathcal{E}_{mn} is the related interaction energy. As a necessary alternative to calculating E

directly for each configuration, we employ the Bragg-Williams approximation which consists of obtaining the average $\langle E \rangle$, for each value of η . Thus

$$\langle E \rangle = - \frac{2}{\Gamma} \sum_{m,n} \mathcal{E}_{mn} \langle N_{mn} \rangle, \quad (2.7)$$

where we have normalized this expression using the coordination number Γ and the factor of 2 because of the two sublattices. Expressions for the $\langle N_{mn} \rangle$ are easily found using the probability factors. For example, $\langle N_{AA} \rangle = (N_A^\alpha)(\Gamma P_A^\beta) = \Gamma N_A^\alpha P_A^\alpha P_A^\beta$. This is a reasonable result since there are N_A^α A atoms on the α lattice, each surrounded by Γ nearest neighbors (which are all elements of the β lattice by construction) whose probability of being another A atom is equal to P_A^β . The others follow similarly, and we find the total average energy becomes

$$\langle E(\eta) \rangle = E(0) - NX_A^2 V_{AB} \eta^2, \quad (2.8)$$

where $E(0)$ is the configurational energy in the completely disordered state and V_{AB} is the ordering energy defined by $V_{AB} = 2\mathcal{E}_{AB} - \mathcal{E}_{AA} - \mathcal{E}_{BB}$. To obtain the temperature dependence of the LRO parameter we minimize the free energy, given by

$$\mathcal{F}(\eta, T) = \mathcal{U}(\eta, T) - T\mathcal{S}(\eta, T). \quad (2.9)$$

When we consider the free energy expressed in terms of the partition function of the ternary system, it follows from a common procedure that the internal energy, $\mathcal{U}(\eta, T)$, is identified with $\langle E(\eta) \rangle$ and the lattice entropy is given by

$$\begin{aligned} \mathcal{S}(\eta, T) &= \frac{Nk_B}{2} (P_A^\alpha \ln P_A^\alpha + P_A^\beta \ln P_A^\beta + P_B^\alpha \ln P_B^\alpha \\ &\quad + P_B^\beta \ln P_B^\beta) - Nk_B X_C \ln X_C, \end{aligned} \quad (2.10)$$

where k_B is the Boltzmann constant. Minimization of \mathcal{F} yields the equilibrium condition

$$\ln \left[\frac{1+f}{1-f} \right] = \frac{4X_A V_{AB} \eta}{k_B T}, \quad (2.11)$$

where $f = (X_A + X_B)\eta / (X_A + X_B \eta^2)$. Taking the limit as $\eta \rightarrow 0$ gives the critical temperature, for any concentration of the three constituents,

$$T_c = \frac{X_A X_B}{X_A + X_B} \frac{2V_{AB}}{k_B}. \quad (2.12)$$

The binary results of Brouers *et al.*¹⁷ correspond to the special case $X_A = X_B$ for which the expressions for f and Eq. (2.11) yield

$$\eta(T) = \tanh \left[\frac{X_A V_{AB} \eta}{k_B T} \right] \quad (2.13)$$

and the critical temperature

$$T_c = \frac{X_A V_{AB}}{k_B}. \quad (2.14)$$

The phase transition is second order, thus, as the temperature is increased past the critical point, the LRO param-

eter smoothly approaches zero. However, as the temperature is decreased below the critical point, the LRO parameter approaches its maximum value of one. Formally speaking, as the critical temperature is approached from above, the system is accompanied by an increase (toward infinity) of some correlation length. In the present case this would simply be the occurrence of an alternating pattern of A and B atoms over larger and larger distances on the lattice.

III. GENERALIZED CPA AND SUBLATTICE ORDERING

This section develops the band-model approach to the order-disorder ternary alloy in the generalized CPA. The periodic and random parts of the alloy Hamiltonian are related to an effective periodic part and scattering corrections, respectively. Since there are two sublattices, two coherent potentials, or equivalently, two electronic self-energies Σ_α and Σ_β are required for this purpose. It results, then, that the periodic part of the Hamiltonian is nondiagonal in the Bloch representation. This complication is overcome by means of a nonunitary transformation connecting the Bloch representation to a diagonal basis in which the formalism simplifies. Vanishing of the average scattering matrix for sublattice α (β) yields a self-consistent equation for Σ_α (Σ_β) and F_α (F_β) where the latter quantity is the diagonal matrix element of the effective periodic Green's function on the bipartite lattice. The alloy density of states is expressed in terms of one-half the sum of F_α and F_β .

We assume that the one-electron alloy Hamiltonian has the tight-binding form

$$H = \sum_{\mathbf{k}} |\mathbf{k}\rangle \varepsilon_{\mathbf{k}} \langle \mathbf{k}| + \sum_n |n\rangle \varepsilon_n \langle n| \quad (3.1)$$

$$\equiv H_0 + V.$$

Here, $|\mathbf{k}\rangle$ represents an electron Bloch state, while the $|n\rangle$ are Wannier states for an electron with energy ε_n . The requirement of two sublattices for the description of ordering necessitates the use of two coherent potentials, U_1 and U_2 . To deal with this mathematically we assume the existence of a vector \mathbf{Q} , defined such that

$$e^{i\mathbf{Q}\cdot\mathbf{R}_n} = \begin{cases} +1, & n \in \alpha \\ -1, & n \in \beta. \end{cases} \quad (3.2)$$

In addition, we require that $\varepsilon_{\mathbf{k}+\mathbf{Q}} = -\varepsilon_{\mathbf{k}}$, which makes the above assumption compatible with a simple cubic or body-centered cubic lattice in the tight-binding approximation. The alloy Hamiltonian is restructured as the sum of an effective periodic part $\tilde{H}_0 = H_0 + U$ and a random perturbing part $\tilde{V} = V - U$ which provides scattering relative to \tilde{H}_0 . We have

$$\tilde{H}_0 = \sum_{\mathbf{k}} |\mathbf{k}\rangle \varepsilon_{\mathbf{k}} \langle \mathbf{k}| + \sum_n |n\rangle (U_1 + U_2 e^{i\mathbf{Q}\cdot\mathbf{R}_n}) \langle n|. \quad (3.3)$$

The coherent potentials, as functions of the complex variable z , obey the reflection property, $U_{1,2}^*(z^*) = U_{1,2}(z)$, and real z will always be taken to mean $z + i\epsilon$ with $\epsilon \rightarrow 0$.

With the above definitions, it is clear that \tilde{H}_0 is not diagonal in the Bloch basis. In fact, it may be written as

$$\tilde{H}_0 = \sum_{\mathbf{k}} |\mathbf{k}\rangle (\varepsilon_{\mathbf{k}} + U_1) \langle \mathbf{k}| + \sum_{\mathbf{k}} |\mathbf{k}\rangle U_2 \langle \mathbf{k} + \mathbf{Q}|. \quad (3.4)$$

The following nonunitary transformations

$$\begin{aligned} |d_{\mathbf{k}}\rangle &= A_{\mathbf{k}} |\mathbf{k}\rangle - B_{\mathbf{k}} |\mathbf{k} + \mathbf{Q}\rangle, \\ |d_{\mathbf{k}+\mathbf{Q}}\rangle &= B_{\mathbf{k}} |\mathbf{k}\rangle + A_{\mathbf{k}} |\mathbf{k} + \mathbf{Q}\rangle, \end{aligned} \quad (3.5)$$

where the transformation coefficients are given by

$$\begin{aligned} A_{\mathbf{k}} &= \frac{1}{\sqrt{2}} \left[1 + \frac{\varepsilon_{\mathbf{k}}}{\sqrt{\varepsilon_{\mathbf{k}}^2 + U_2^2}} \right]^{1/2}, \\ B_{\mathbf{k}} &= \frac{1}{\sqrt{2}} \frac{\varepsilon_{\mathbf{k}}}{|\varepsilon_{\mathbf{k}}|} \left[1 - \frac{\varepsilon_{\mathbf{k}}}{\sqrt{\varepsilon_{\mathbf{k}}^2 + U_2^2}} \right]^{1/2}, \end{aligned} \quad (3.6)$$

diagonalize the effective periodic Hamiltonian:

$$\tilde{H}_0 = \sum_{\mathbf{k}} |d_{\mathbf{k}}\rangle \left[\frac{\varepsilon_{\mathbf{k}}}{|\varepsilon_{\mathbf{k}}|} \sqrt{\varepsilon_{\mathbf{k}}^2 + U_2^2} + U_1 \right] \langle d_{\mathbf{k}}|, \quad (3.7)$$

where the quantity in parentheses shall henceforth be called $E_{\mathbf{k}}$.

Calculation of the configurational average alloy Green's function $\langle G(z) \rangle$ with the CPA is facilitated by the methods of multiple scattering theory. In that formalism, an average total scattering operator $\langle T \rangle$ is defined by the relation

$$\langle G(z) \rangle = \tilde{G}_0(z) + \tilde{G}_0(z) \langle T \rangle \tilde{G}_0(z). \quad (3.8)$$

Here, $\tilde{G}_0(z)$ is the Green's function of the effective periodic Hamiltonian \tilde{H}_0 . The scattering operator may be expressed in terms of itself in a standard way by

$$T = \tilde{V} + \tilde{V} \tilde{G}_0 T. \quad (3.9)$$

Iteration of Eq. (3.9) leads to an infinite series for T in terms of \tilde{G}_0 and the random perturbation \tilde{V} . The CPA takes the viewpoint that the vanishing of $\langle T \rangle$ is a self-consistent condition for the unknown U . In this way, the second term on the right-hand side of Eq. (3.8) makes no contribution and $\langle G(z) \rangle$ coincides with \tilde{G}_0 . Because \tilde{V} assumes the form of a sum of localized site contributions, it follows that T may be written as the sum of contributions T_n due to individual sites. In the single-site approximation, the vanishing of $\langle T \rangle$ is equivalent to requiring that $\langle \tilde{t}_n \rangle = 0$ since $\langle T_n \rangle$ may be shown to be a product of $\langle \tilde{t}_n \rangle$, the average atomic transition operator for the n th site, and an average effective wave originating from all other sites.

Application of the basic CPA procedure to each sublattice independently yields equations for the determination of the coherent potentials U_1 and U_2 . We obtain

$$\begin{aligned} P_A^\alpha t_A + P_B^\alpha t_B + P_C^\alpha t_C &= 0, \\ P_A^\beta t_A + P_B^\beta t_B + P_C^\beta t_C &= 0. \end{aligned} \quad (3.10)$$

The t_n in Eqs. (3.10) are matrix elements of \tilde{t}_n in the Wannier representation. Explicitly, the latter quantity is found to be (with $n \in \{A, B, C\}$)

$$\tilde{r}_n = |n\rangle (\epsilon_n - U_1 - U_2 e^{iQ \cdot R_n}) [1 - (\epsilon_n - U_1 - U_2 e^{iQ \cdot R_n}) F_n]^{-1} \langle n| . \quad (3.11)$$

The diagonal effective Green's functions $F_n(z)$ are given by

$$F_n(z) = \langle n | (z - \tilde{H}_0)^{-1} | n \rangle = (z - U_1 + U_2 e^{iQ \cdot R_n}) \frac{1}{N} \sum_k [(z - U_1)^2 - U_2^2 - \epsilon_k^2]^{-1} , \quad (3.12)$$

where, now, $n \in \{\alpha, \beta\}$. In terms of the self-energies, $\Sigma_\alpha = U_1 + U_2$ and $\Sigma_\beta = U_1 - U_2$, Eq. (3.10) yields a system of two, nonlinear complex equations:

$$\Sigma_\alpha^3 F_\alpha^2 - \epsilon_{BC} \Sigma_\alpha^2 F_\alpha^2 + 2 \Sigma_\alpha^2 F_\alpha + \epsilon_B \epsilon_C \Sigma_\alpha F_\alpha^2 - (\epsilon_{BC} + \epsilon_\alpha) \Sigma_\alpha F_\alpha + \Sigma_\alpha + P_{BC}^\alpha \epsilon_B \epsilon_C F_\alpha - \epsilon_\alpha = 0 \quad (3.13a)$$

and

$$\Sigma_\beta^3 F_\beta^2 - \epsilon_{BC} \Sigma_\beta^2 F_\beta^2 + 2 \Sigma_\beta^2 F_\beta + \epsilon_B \epsilon_C \Sigma_\beta F_\beta^2 - (\epsilon_{BC} + \epsilon_\beta) \Sigma_\beta F_\beta + \Sigma_\beta + P_{BC}^\beta \epsilon_B \epsilon_C F_\beta - \epsilon_\beta = 0 , \quad (3.13b)$$

where we have defined, for convenience,

$$\begin{aligned} \epsilon_{BC} &= \epsilon_B + \epsilon_C , \\ \epsilon_{\alpha, \beta} &= P_B^{\alpha, \beta} \epsilon_B + P_C^{\alpha, \beta} \epsilon_C , \\ P_{BC}^{\alpha, \beta} &= P_B^{\alpha, \beta} + P_C^{\alpha, \beta} . \end{aligned} \quad (3.14)$$

Use of the Hubbard, semicircular model DOS given by¹⁸

$$g_0(z) = \begin{cases} \frac{2}{\pi} (1 - z^2)^{1/2}, & |z| \leq 1 \\ 0, & |z| \geq 1 , \end{cases} \quad (3.15)$$

yields, for the F functions,

$$F_0(z) = 2[z - (z^2 - 1)^{1/2}] \quad (3.16)$$

and

$$F_\alpha = (z - \Sigma_\beta) \frac{F_0(\xi)}{\xi} , \quad F_\beta = (z - \Sigma_\alpha) \frac{F_0(\xi)}{\xi} , \quad (3.17)$$

with $\xi^2 = (z - \Sigma_\alpha)(z - \Sigma_\beta)$. Equations (3.13) and (3.17) show that the α and β sublattice variables are coupled. As in the case of the disordered ternary alloy, to obtain a form useful for numerical solutions, we eliminate the self-energies in favor of the F functions which satisfy two, coupled fifth-order nonlinear complex equations. For further numerical simplicity, these equations are expressed in terms of new variables F_+ and F_- given by one-half the sum and difference of F_α and F_β respectively. The alloy density of electron states is related to the former quantity by

$$g(E) = -\frac{1}{\pi} \text{Im} F_+(E) . \quad (3.18)$$

Equations (3.13) are reminiscent of the mixed polynomial in F and the self-energy Σ of the disordered ternary alloy on a single lattice. Indeed, when the LRO parameter vanishes, the entire formalism reduces to this limiting case where F_- and F_+ become zero and F , respectively, and the α and β self-energies coincide with Σ .

IV. MOMENTS OF THE DOS AND TEMPERATURE DEPENDENCE OF THE LRO PARAMETER

This section provides a band-model calculation of the temperature dependence of the LRO parameter. For this

purpose we consider values of the B -atom energy ϵ_B greater than 2. This allows us to approximate the electronic free energy through the use of moments of the ternary alloy density of states. Although we obtain an asymptotic form for the temperature dependence, the results coincide with those found in the Bragg-Williams approach.

In general, we define the moments of the DOS by¹⁹

$$\mu_p = \int_{-\infty}^{\infty} dz z^p g(z) = \frac{1}{N} \text{Tr} \langle H^p \rangle . \quad (4.1)$$

The reference crystal moments, $\mu_p^{(0)}$, are similarly defined by replacing $g(z)$ and H by $g_0(z)$ and H_0 , respectively, in the above expression. In particular, if the reference crystal DOS, $g_0(z)$ is symmetric, then $\mu_p^{(0)}$ vanishes for odd values of p . For the order-disorder ternary alloy, the relevant moments⁸ are, with the exception of the tilde-term in Eq. (4.2) which contains the LRO parameter,

$$\begin{aligned} \mu_0 &= 1, \quad \mu_1 = \Delta_1, \quad \mu_2 = \Delta_2 + \mu_2^{(0)} , \\ \mu_3 &= \Delta_3 + 3\Delta_1 \mu_2^{(0)} , \\ \mu_4 &= \Delta_4 + 4\Delta_2 \mu_2^{(0)} + 2\tilde{\Delta}_1^2 \mu_2^{(0)} + \mu_4^{(0)} , \end{aligned} \quad (4.2)$$

where

$$\begin{aligned} \Delta_p &= X_A \epsilon_A + X_B \epsilon_B + X_C \epsilon_C , \\ \tilde{\Delta}_1^2 &= \Delta_1^2 - X_A^2 (\epsilon_A - \epsilon_B)^2 \eta^2 . \end{aligned} \quad (4.3)$$

When $|\epsilon_B|$ is much larger than $\max \epsilon_k - \min \epsilon_k$, two well-defined, nonintersecting regions are formed. One centered around ϵ_B and the other around $\epsilon = (X_A \epsilon_A + X_C \epsilon_C) (X_A + X_C)^{-1}$, the center of gravity of the A and C atom energies. This is called the singly split band limit of the alloy. A doubly split band limit also exists for the ternary alloy but it does not affect the LRO-dependent terms that we wish to consider. We now write the DOS as a sum of two parts: a lower subband and an upper subband. Thus $g(z) = g_L(z) + g_U(z)$, which allows us to express the moments as

$$\begin{aligned}
\mu_p &= \int_{-\infty}^{\infty} dz z^p g(z) \\
&= \int_{-\infty}^{\infty} dz (z - \varepsilon_B + \varepsilon_B)^p g_L(z) \\
&\quad + \int_{-\infty}^{\infty} dz (z - \varepsilon + \varepsilon)^p g_U(z) \\
&= \sum_{l=0}^p \binom{p}{l} [\varepsilon_B^l \mu_p^L - l + \varepsilon^l \mu_p^U - l] .
\end{aligned} \tag{4.4}$$

Here, we have used the binomial expansion and defined the moments relative to the subbands by

$$\begin{aligned}
\mu_p^L &= \int_{-\infty}^{\infty} dz (z - \varepsilon_B)^p g_L(z) , \\
\mu_p^U &= \int_{-\infty}^{\infty} dz (z - \varepsilon)^p g_U(z) .
\end{aligned} \tag{4.5}$$

The infinite set of equations resulting from Eq. (4.4) must be solved by truncation. However, one runs into the apparent problem of having twice as many variables (μ_p^L and μ_p^U) as there are equations. This difficulty is resolved by recognizing that, for large ε_B , only its highest powers in the expressions are significant. In our case we will systematically neglect all terms of order ε_B^{-3} and higher. Using the moment expressions obtained in Eq. (4.2) we find

$$\mu_0^L = X_B, \quad \mu_1^L = X_B(1 - X_B)\mu_2^{(0)}\varepsilon_B^{-1} + X_A^2\eta^2\mu_2^{(0)}\varepsilon_B^{-1}, \tag{4.6}$$

which is all we require for the subsequent analysis.

The electronic free energy may be written

$$\mathcal{F}_{el}(\eta, T) = -\frac{N}{\beta} \int_{-\infty}^{\infty} dz g(z) \ln(1 + e^{-\beta z}) . \tag{4.7}$$

At temperatures such that $k_B T \ll |\varepsilon_B|$, the lower subband is full while the upper subband remains empty. This permits us to approximate the free energy by

$$\begin{aligned}
\mathcal{F}_{el}(\eta, T) &\approx N \int_{-\infty}^{\infty} dz g_L(z) + O(e^{-\beta|\varepsilon_B|}) \\
&= N \int_{-\infty}^{\infty} dz (z + |\varepsilon_B|) g_L(z) \\
&\quad - N|\varepsilon_B| \int_{-\infty}^{\infty} dz g_L(z) \\
&= N\mu_1^L - N|\varepsilon_B|\mu_0^L .
\end{aligned} \tag{4.8}$$

Substitution of the expressions for μ_0^L and μ_1^L into Eq. (4.8) yields

$$\mathcal{F}_{el} = \mathcal{U}(0) - NX_A^2\mu_2^{(0)}\eta^2|\varepsilon_B|^{-1}, \tag{4.9}$$

where $\mathcal{U}(0) = -N[X_B(1 - X_B)\mu_2^{(0)}|\varepsilon_B|^{-1} + X_B|\varepsilon_B|]$. Comparison of this result for the electronic free energy with the Bragg-Williams form of the average configurational energy [Eq. (2.8)] shows that the association

$$\mu_2^{(0)}|\varepsilon_B|^{-1} = V_{AB}, \tag{4.10}$$

brings these two quantities into coincidence. The critical temperature may now be written as

$$T_c = \frac{X_A X_B}{X_A + X_B} \frac{2\mu_2^{(0)}}{k_B |\varepsilon_B|} . \tag{4.11}$$

This result reduces to that of Plischke and Mattis when the A and B atom concentrations are equal.

V. ELECTRICAL CONDUCTIVITY AND ORDER-DISORDER ON A BIPARTITE LATTICE WITH CUBIC SYMMETRY

In this section we employ the generalized CPA to study the dc electrical conductivity of the order-disorder ternary alloy. This application follows previous^{14,20} calculations of the transport properties of disordered alloys in the single-site approximation. The ordering effect is incorporated, as in the binary case,¹⁰ by making use of complex transformations that diagonalize the one-electron Green's function. The conductivity is expressed in terms of two integrals which may be evaluated in closed form by contour integration in the complex energy plane. The analytical results are identical with those reported for the disordered binary alloy,²⁰ except that the input self-energy is specific to the order-disorder ternary alloy.

We begin by introducing the well-known Greenwood-Peierls^{21,22} formula for the electrical-conductivity tensor:

$$\sigma_{\mu\nu} = \frac{2e^2\hbar\pi}{m^2\Omega} \int dE \left[-\frac{df}{dE} \right] \text{Tr} \langle p_\mu \delta(E - H) p_\nu \delta(E - H) \rangle , \tag{5.1}$$

with μ and ν representing cartesian coordinates. This closed formal expression for $\sigma_{\mu\nu}$ is the result of calculating the current density to first order in the applied electric field. Kubo²³ has given a more general expression for $\sigma_{\mu\nu}$ which reduces to Eq. (5.1) for the case of a noninteracting electron gas at zero temperature, as shown by Verboven.²⁴ Here, H is the alloy Hamiltonian of Eq. (3.1), f denotes the Fermi function, e and m are the electron charge and mass, respectively. Ω is the crystal volume, and p_μ are components of the linear momentum. The prefactor of 2 takes into account the two spin states of the electron. The angular brackets denote the configurational average. The following procedure parallels Ref. 5 in showing that vertex corrections to the electrical conductivity vanish in the order-disorder ternary model. These corrections were first found to vanish for both the disordered binary²⁰ and ternary¹⁴ cases. The alloy Hamiltonian H and therefore its corresponding Green's function G , are not diagonal in the Bloch representation. Thus, in general, the Green's function matrix elements connect different sublattices, making zero vertex corrections not an immediately obvious result.

It follows from the definition of the alloy Green's function that

$$G(E^-) - G(E^+) = 2\pi i \delta(E - H), \tag{5.2}$$

where E^\pm is an abbreviation for $E \pm i\epsilon$. By applying this identity to Eq. (5.1), the conductivity tensor may be given the compact form

$$\sigma_{\mu\nu} = \frac{2e^2\hbar\pi}{m^2\Omega} \int dE \left[-\frac{df}{dE} \right] I_{\mu\nu}(E) . \tag{5.3}$$

The quantities $I_{\mu\nu}(E)$ have the expression

$$I_{\mu\nu}(E) = \frac{1}{4\pi^2} \text{Tr} \{ p_\mu [K_\nu(E^+, E^-) + K_\nu(E^-, E^+) - K_\nu(E^+, E^+) - K_\nu(E^-, E^-)] \}, \quad (5.4)$$

where the K_ν are terms of the form

$$K_\nu(z, z') = \langle G(z) p_\nu G(z') \rangle, \quad (5.5)$$

which describe the averaged propagation of two electrons, or in other words, the motion of correlated electron pairs. Many of the following results, in reducing K_ν , may also be derived on the basis of more elegant functional techniques.²⁵ These make use of an alternate form of the Green's function, in terms of the random potential, as a starting point. The procedure here is more traditional. First, we recall from Eq. (3.8) that $G(z)$ may be conveniently expressed without the averaging brackets as

$$G(z) = \bar{G}(z) + \bar{G}(z) T \bar{G}(z). \quad (5.6)$$

Combining Eqs. (5.5) and (5.6), and invoking the CPA condition, we find that K_ν becomes

$$K_\nu(z, z') = \bar{G} p_\nu \bar{G}' + \bar{G} \Gamma_\nu(z, z') \bar{G}', \quad (5.7)$$

where \bar{G} is short for $\langle G \rangle$. The complex energy variables z and z' have been suppressed in \bar{G} and \bar{G}' , respectively. The quantity Γ_ν defines the function which gives rise to

vertex corrections due to simultaneous averaging of both Green's functions in Eq. (5.7). On the other hand, the first term on the right-hand side of Eq. (5.7) comes from independent averagings. The determination of K_ν now rests on an approximation for the vertex correction,

$$\Gamma_\nu(z, z') = \langle T \bar{G} p_\nu \bar{G}' T' \rangle, \quad (5.8)$$

consistent with the development of the electron self-energy and \bar{G} on the bipartite lattice.

By repeated use of the single-site approximation we systematically reduce the vertex term to a sum of expressions involving the atomic scattering operator \tilde{t}_n . The result is

$$\Gamma_\nu(z, z') = \sum_n \langle \tilde{t}_n \bar{G} p_\nu \bar{G}' \tilde{t}_n' \rangle + \sum_n \sum_{m \neq n} \langle \tilde{t}_n \bar{G} \langle \tilde{t}_m \bar{G} p_\nu \bar{G}' \tilde{t}_m' \rangle \bar{G}' \tilde{t}_n' \rangle + \dots \quad (5.9)$$

The single-site approximation is maintained by averaging after each step in the series. The exclusions in the sum represent an absence of two electrons returning to the same site. Clearly, evaluation of the vertex equation requires us to deal with the common term $\langle \tilde{t}_n \bar{G} p_\nu \bar{G}' \tilde{t}_n' \rangle$. Writing the scattering matrix explicitly as an operator in the Wannier representation (i.e., $\tilde{t}_n = |n\rangle t_n \langle n|$) we find

$$\begin{aligned} \langle \tilde{t}_n \bar{G} p_\nu \bar{G}' \tilde{t}_n' \rangle &= |n\rangle \{ \langle t_n \langle n | \bar{G} p_\nu \bar{G}' | n \rangle t_n' \rangle \} \langle n | \\ &= |n\rangle \langle t_n \sum_{m,l} \langle n | \bar{G} | m \rangle \langle m | p_\nu | l \rangle \langle l | \bar{G}' | n \rangle t_n' \rangle \langle n |. \end{aligned} \quad (5.10)$$

Evaluation of the matrix elements of the Green's function in Eq. (5.10) requires some care since it is not diagonal in the Bloch basis. However, we may insert a complete set of the diagonal basis introduced in Eqs. (3.5) and (3.6). The result is

$$\begin{aligned} \langle n | \bar{G} p_\nu \bar{G}' | n \rangle &= \frac{1}{N^3} \sum_{m,l} \sum_{\mathbf{k}} e^{i\mathbf{k} \cdot (\mathbf{R}_m - \mathbf{R}_l)} p_\nu(\mathbf{k}) \sum_{\mathbf{k}_1} e^{i\mathbf{k}_1 \cdot (\mathbf{R}_n - \mathbf{R}_m)} M(\mathbf{k}_1, \mathbf{R}_n) M(\mathbf{k}_1, \mathbf{R}_n) M(\mathbf{k}_1, \mathbf{R}_m) (z - E_{\mathbf{k}_1})^{-1} \\ &\quad \times \sum_{\mathbf{k}_2} e^{i\mathbf{k}_2 \cdot (\mathbf{R}_l - \mathbf{R}_n)} M(\mathbf{k}_2, \mathbf{R}_l) M(\mathbf{k}_2, \mathbf{R}_n) (z - E_{\mathbf{k}_2})^{-1}. \end{aligned} \quad (5.11)$$

Here, we have defined, for convenience, $M(\mathbf{k}, \mathbf{R}_n) = (A_{\mathbf{k}} - B_{\mathbf{k}} e^{i\mathbf{Q} \cdot \mathbf{R}_n})$. The momentum matrix elements are

$$\langle m | p_\nu | l \rangle = \frac{1}{N} \sum_{\mathbf{k}} e^{i\mathbf{k} \cdot (\mathbf{R}_m - \mathbf{R}_l)} p_\nu(\mathbf{k}) \quad (5.12)$$

and $p_\nu(\mathbf{k}) = \langle \mathbf{k} | p_\nu | \mathbf{k} \rangle$. The transformation coefficients $A_{\mathbf{k}}$ and $B_{\mathbf{k}}$, and the dispersion formula $E_{\mathbf{k}}$ only depend on \mathbf{k} through $\varepsilon_{\mathbf{k}}$. In view of the fact that the velocity $v(\mathbf{k})$ and $\varepsilon_{\mathbf{k}}$ are antisymmetric and symmetric, respectively, under time reversal,²⁶ we find that the entire expression of Eq. (5.11) vanishes. This remarkable simplification also means that the vertex term vanishes and we are left with the simple result that $K_\nu(z, z')$ is equal to the first term on the right-hand side of Eq. (5.7).

Going back to the trace expression in Eq. (5.4), we must now obtain, explicitly, terms of the form

$$\text{Tr}(p_\mu K_\nu) = \text{Tr}(p_\mu \bar{G} p_\nu \bar{G}') = \sum_{\mathbf{k}} \sum_{\mathbf{k}'} p_\mu(\mathbf{k}) p_\nu(\mathbf{k}') \langle \mathbf{k} | \bar{G} | \mathbf{k}' \rangle \langle \mathbf{k}' | \bar{G}' | \mathbf{k} \rangle. \quad (5.13)$$

Once again, insertion of the diagonalized basis on the Green's functions gives

$$\langle \mathbf{k} | \bar{G} | \mathbf{k}' \rangle = (A_{\mathbf{k}} A_{\mathbf{k}'} G_{\mathbf{k}} + B_{\mathbf{k}} B_{\mathbf{k}'} Q_{\mathbf{k}}) \delta_{\mathbf{k}, \mathbf{k}'} + B_{\mathbf{k}} A_{\mathbf{k}'} G_{\mathbf{k}'} \delta_{\mathbf{k}, \mathbf{k}'+\mathbf{Q}} + A_{\mathbf{k}} B_{\mathbf{k}'} G_{\mathbf{k}} \delta_{\mathbf{k}, \mathbf{k}'+\mathbf{Q}}, \quad (5.14)$$

where we have defined

$$G_{\mathbf{k}} = \langle d_{\mathbf{k}} | \bar{G} | d_{\mathbf{k}} \rangle = \left[\lambda - \frac{\varepsilon_{\mathbf{k}}}{|\varepsilon_{\mathbf{k}}|} \rho \right]^{-1}, \quad Q_{\mathbf{k}} = \langle d_{\mathbf{k}+\mathbf{Q}} | \bar{G} | d_{\mathbf{k}+\mathbf{Q}} \rangle = \left[\lambda + \frac{\varepsilon_{\mathbf{k}}}{|\varepsilon_{\mathbf{k}}|} \rho \right]^{-1}, \quad (5.15)$$

and $\lambda = z - U_1$, $\rho = (\varepsilon_{\mathbf{k}}^2 + U_2^2)^{1/2}$. Substitution of the Green's function matrix elements into Eq. (5.13) then gives

$$\text{Tr}(p_{\mu} K_{\nu}) = \sum_{\mathbf{k}} p_{\mu}(\mathbf{k}) p_{\nu}(\mathbf{k}) [(A_{\mathbf{k}}^2 G_{\mathbf{k}} + B_{\mathbf{k}}^2 Q_{\mathbf{k}})(A_{\mathbf{k}}'^2 G_{\mathbf{k}}' + B_{\mathbf{k}}'^2 Q_{\mathbf{k}}') - A_{\mathbf{k}} B_{\mathbf{k}}(G_{\mathbf{k}} - Q_{\mathbf{k}}) A_{\mathbf{k}}' B_{\mathbf{k}}'(G_{\mathbf{k}}' - Q_{\mathbf{k}}')] . \quad (5.16)$$

We may combine all four terms in the trace expression to give the conductivity of Eq. (5.3) the form

$$\sigma_{\mu\nu} = \frac{2e^2 \hbar}{\pi \Omega} \int dE \left[-\frac{df}{dE} \right] \sum_{\mathbf{k}} v_{\mu}(\mathbf{k}) v_{\nu}(\mathbf{k}) [\text{Im}^2(A_{\mathbf{k}}^2 G_{\mathbf{k}} + B_{\mathbf{k}}^2 Q_{\mathbf{k}}) - \text{Im}^2 A_{\mathbf{k}} B_{\mathbf{k}}(G_{\mathbf{k}} - Q_{\mathbf{k}})] , \quad (5.17)$$

where use has been made of the identity $\text{Im}^2 f = \frac{1}{4}(f - f^*)^2$ and all points are now taken at $z = E + i\epsilon$.

In an effort to simplify Eq. (5.17) we introduce the following function:

$$\Phi_{\mu\nu}(\xi) = \frac{1}{N} \sum_{\mathbf{k}} v_{\mu}(\mathbf{k}) v_{\nu}(\mathbf{k}) \delta(\xi - \varepsilon_{\mathbf{k}}) . \quad (5.18)$$

This permits us to write the conductivity as

$$\sigma_{\mu\nu} = \frac{2e^2 \hbar}{\pi \Omega_c} \int dE \left[-\frac{df}{dE} \right] \int d\xi \Phi_{\mu\nu}(\xi) L(\xi) , \quad (5.19)$$

where $\Omega_c = \Omega/N$ and $L(\xi) = [\text{Im}(A^2 G + B^2 Q)]^2 - [\text{Im} AB(G - Q)]^2$. We may further reduce the results by using the density-of-states expression

$$g_0(\xi) = \frac{1}{N} \sum_{\mathbf{k}} \delta(\xi - \varepsilon_{\mathbf{k}}) , \quad (5.20)$$

and constructing the average squared velocity

$$v^2(\xi) = [g_0(\xi)]^{-1} \sum_{\mathbf{k}} v^2(\mathbf{k}) \delta(\xi - \varepsilon_{\mathbf{k}}) . \quad (5.21)$$

For systems with cubic symmetry, these results may be combined to reexpress Eq. (5.18) as

$$\begin{aligned} \Phi_{\mu\nu}(\xi) &= \frac{1}{3N} \sum_{\mathbf{k}} v^2(\mathbf{k}) \delta(\xi - \varepsilon_{\mathbf{k}}) \delta_{\mu\nu} \\ &= \frac{1}{3} g_0(\xi) v^2(\xi) \delta_{\mu\nu} . \end{aligned} \quad (5.22)$$

Upon using the semicircular model DOS for $g_0(\xi)$ and the Velicky expression for the squared velocity term²⁰ we

$$\begin{aligned} J_2(E) &= \frac{\pi}{4|C|^3} r^{-1/2} \rho^{1/2} \left\{ |C| \left[(2 - 5B) \sin \left[\frac{\psi - \phi}{2} \right] - 5|C| \cos \left[\frac{\psi - \phi}{2} \right] \right] + \rho \left[2B \cos \left[\frac{3\psi - \phi}{2} \right] \right. \right. \\ &\quad \left. \left. - 3|C| \sin \left[\frac{3\psi - \phi}{2} \right] \right] \right\} , \end{aligned} \quad (5.26b)$$

where we have made the definitions

$$\begin{aligned} r &= (B^2 + C^2)^{1/2}, \quad \rho = [(1 - B^2)^2 + C^2]^{1/2}, \\ \tan \psi &= \frac{|C|}{B - 1}, \quad -\pi \leq \psi \leq 0, \\ \tan \phi &= \frac{|C|}{B}, \quad 0 \leq \phi \leq \pi. \end{aligned} \quad (5.27)$$

finally have

$$\Phi_{\mu\nu} = \frac{2v_m^2}{3\pi} (1 - \xi^2)^{3/2} \delta_{\mu\nu} , \quad (5.23)$$

where v_m is the maximum velocity in the band. By inserting the expressions for $\Phi_{\mu\nu}(\xi)$ and $L(\xi)$ into the preceding form of the conductivity, and using the approximation that replaces the negative energy derivative of the Fermi function by a δ function centered at the Fermi energy, it follows that

$$\sigma = \sigma_0 [AJ_1(E) + 8C^2 J_2(E)] , \quad (5.24)$$

where $\sigma_0 = e^2 v_m \hbar / 3\pi^2 \Omega_c$. The quantities J_1 and J_2 are given by the integrals

$$\begin{aligned} J_1(E) &= \int_{-1}^{+1} d\xi \frac{(1 - \xi^2)^{3/2}}{(B - \xi^2)^2 + C^2} , \\ J_2(E) &= \int_{-1}^{+1} d\xi \frac{(1 - \xi^2)^{3/2}}{[(B - \xi^2)^2 + C^2]^2} , \end{aligned} \quad (5.25)$$

with $A = 4 \text{Im}(\Sigma_{\alpha}) \text{Im}(\Sigma_{\beta})$, $B = \text{Re}(z - \Sigma_{\alpha})(z - \Sigma_{\beta})$, $C = \text{Im}(z - \Sigma_{\alpha})(z - \Sigma_{\beta})$. Evaluation of the above integrals may be done in closed form by performing contour integrations in the complex plane. With branch points at $\xi = \pm 1$ we find

$$J_1(E) = \pi + \frac{\pi}{|C|} r^{-1/2} \rho^{3/2} \cos \left[\frac{3\psi - \phi}{2} \right] \quad (5.26a)$$

and

At this point, it is straightforward, although tedious, to show that Eq. (5.24) reduces to the expression for σ of the disordered ternary alloy when the LRO parameter vanishes. Actually, Eq. (5.17) is a more convenient point at which this limiting case may be realized with $U_2 = 0$, $A_{\mathbf{k}} = 1$, and $B_{\mathbf{k}} = 0$. Numerical examples of the DOS and conductivity versus energy plots are presented in the following section.

VI. NUMERICAL RESULTS

The solution of the coupled equations in F_α and F_β was accomplished using a routine in the International Mathematical and Statistical Libraries, Inc. (IMSL) called NEQNJ. This solves n coupled nonlinear complex equations with a user-supplied Jacobian. To fully characterize the alloy we require, as input parameters, the concentrations X_B and X_C ; the scattering strengths ϵ_B and ϵ_C (recall, $\epsilon_A=0$); and the order parameter, η . To reduce

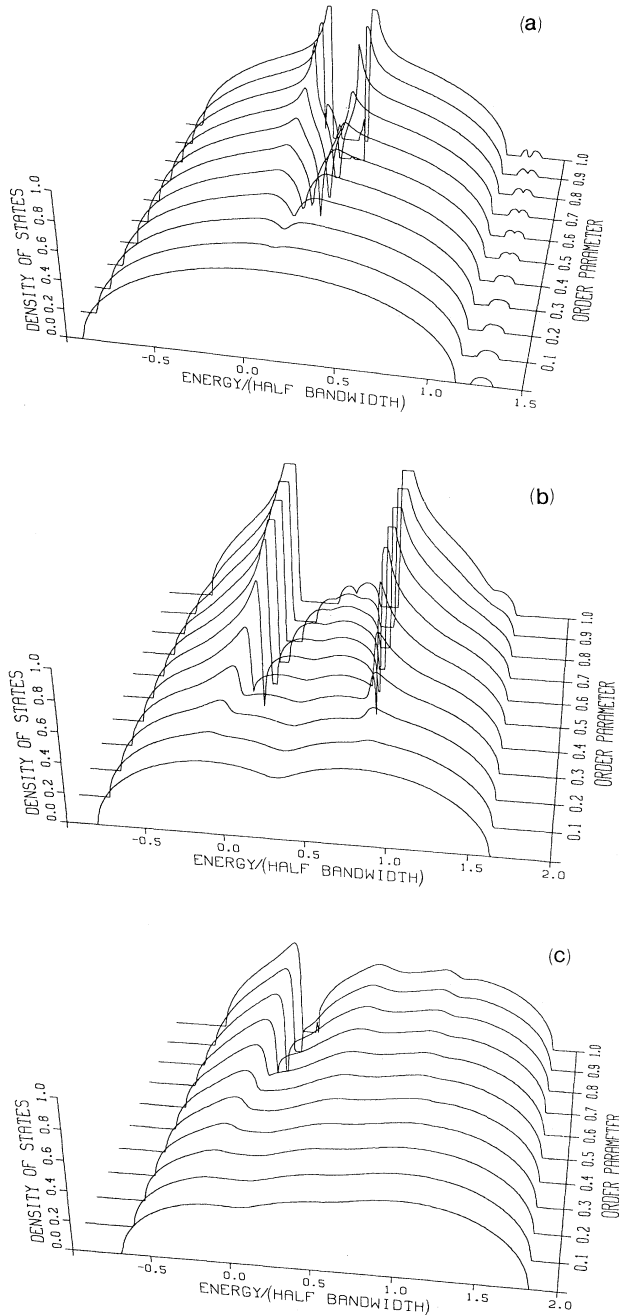


FIG. 1. Density of states as a function of energy and ordering with (a) $X_C=0.005$, $X_B=0.48$, $\epsilon_B=0.25$; (b) $X_C=0.05$, $X_B=0.49$, $\epsilon_B=0.75$; (c) $X_C=0.50$, $X_B=0.25$, $\epsilon_B=0.50$.

this wide range of choices, we have selected $\epsilon_C=1$ throughout and used $X_C=0.005$, 0.05 , and 0.50 as a fairly representative range of the effect of the C -atom concentration on the DOS and conductivity. Also, the value of the B -atom concentration is usually chosen to be as close to an even mixture with the A atom as the numerics will allow. This is done because only the A and B atoms are involved in the ordering process and the effects of this ordering are most pronounced when the two concentrations are equal.

In Figs. 1(a)–1(c) and 4(a)–4(c) the front graph corresponds to the completely disordered ternary case (i.e., order parameter, $\eta=0$). An increase in ordering is then found by moving “inward” until the maximum is attained ($\eta=1$). The energy axis is in units of the half-bandwidths of the reference crystal. Figure 1(a) represents a DOS for a C -atom concentration of 0.005 and hence, it is this graph that most closely resembles binary alloy results. In particular, a valley, in the center of the band, begins to form and becomes more pronounced as order is increased. At $\eta=1$, the DOS is almost zero over the range bounded by the A -atom potential ($\epsilon_A=0$) and the B -atom potential ($\epsilon_B=0.25$, in this case). The only exceptions are two small band structures due in part to the fact that we do not have a perfectly even mixture of A and B atoms and in part to the random presence of the C atom. Perhaps the most obvious new feature the third atom introduces at these concentrations is the small satellite band to the right of the larger band. It also shows the development of a valley as order is increased. Figure 4(a) is the corresponding conductivity and it is plotted as a function of Fermi energy and ordering parameter. The conductivity shows the same characteristic shape as the DOS—the formation of a valley at the center accompanied by an increase in the conductivity on either side of

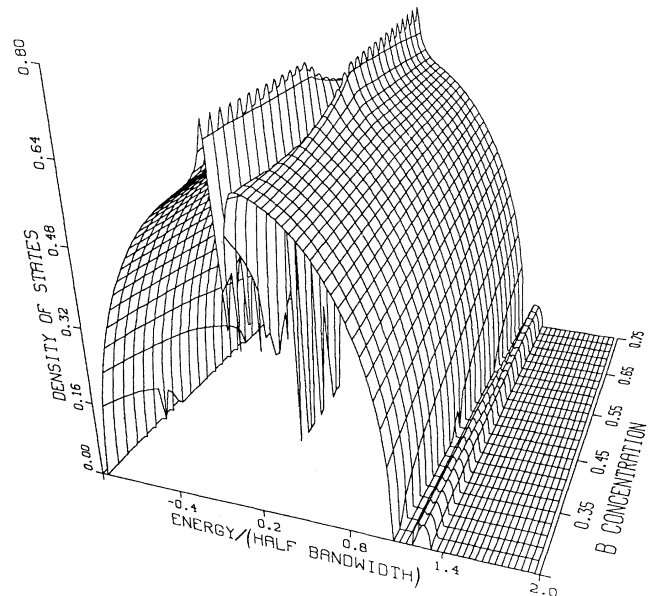


FIG. 2. Density of states as a function of energy and B -atom concentration. $\epsilon_B=0.25$; $\eta=0.60$.

this valley. The absence of the smaller satellite is due to the resolution of the numbers. Since the Fermi energy is related to the electron concentration, these plots may be thought of as revealing variations of the conductivity for different electron concentrations.

Figure 1(b) shows a DOS for a C -atom concentration of 0.05, a B -atom potential of 0.75, and a B -atom concentration of 0.49. At this energy the larger band has essentially enveloped the smaller band making its presence all but invisible except at $\eta=1$. In this case, as η approaches 1, the central part of the valley begins to reveal more structure than the previous case. As before, at perfect order, the small band structures in the center of the valley are there because of the unavoidable overlap of B atoms on the α lattice and because of the C atom (the two humps are of different sizes). Similarly, Fig. 4(b) is the conductivity associated with the above parameters. Note the change in scale; the overall conductivity is lower since there are now more (random) C atoms.

Figure 1(c) is a DOS plot with a C -atom concentration of 0.5 and equal concentrations of A and B atoms at 0.25; the B -atom energy is 0.50. The major part of the band is now primarily around the C -atom energy of 1.00 and hence, a much smaller valley forms as order is increased among the A and B atoms. This, of course, is due to the greater dominance of the C atom. Again, Fig. 4(c) is the corresponding conductivity however, the scale now is

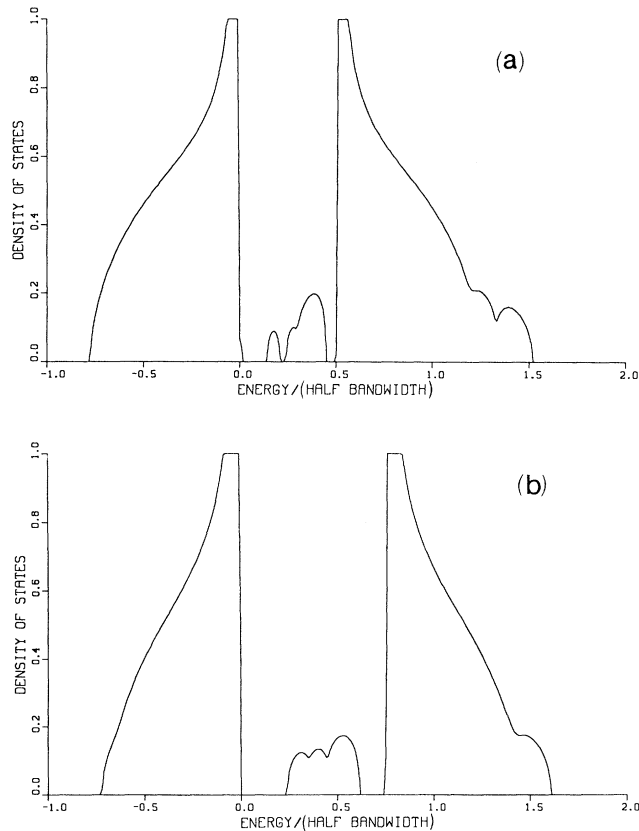


FIG. 3. Density of states as a function of energy. The order parameter is set at (a) $\eta=0.98$ and $X_C=0.05$, $X_B=0.475$, $\epsilon_B=0.50$; (b) $\eta=0.95$ and $X_C=0.05$, $X_B=0.475$, $\epsilon_B=0.75$.

only up to 100. As we mentioned before, this overall decrease in the conductivity is to be expected when we increase the C -atom concentration since the element of disorder has been increased.

Figures 3(a) and 3(b) show plots of the DOS with a C -atom concentration of 0.05. Both of the graphs use equal concentrations of A and B atoms (0.475) as input parameters. In particular, Fig. 3(a) uses a B -atom energy at 0.50 and the order parameter is set at 0.98. Inside the valley (for both figures) the small, left-hand band structure and the little notch in the right-hand structure are

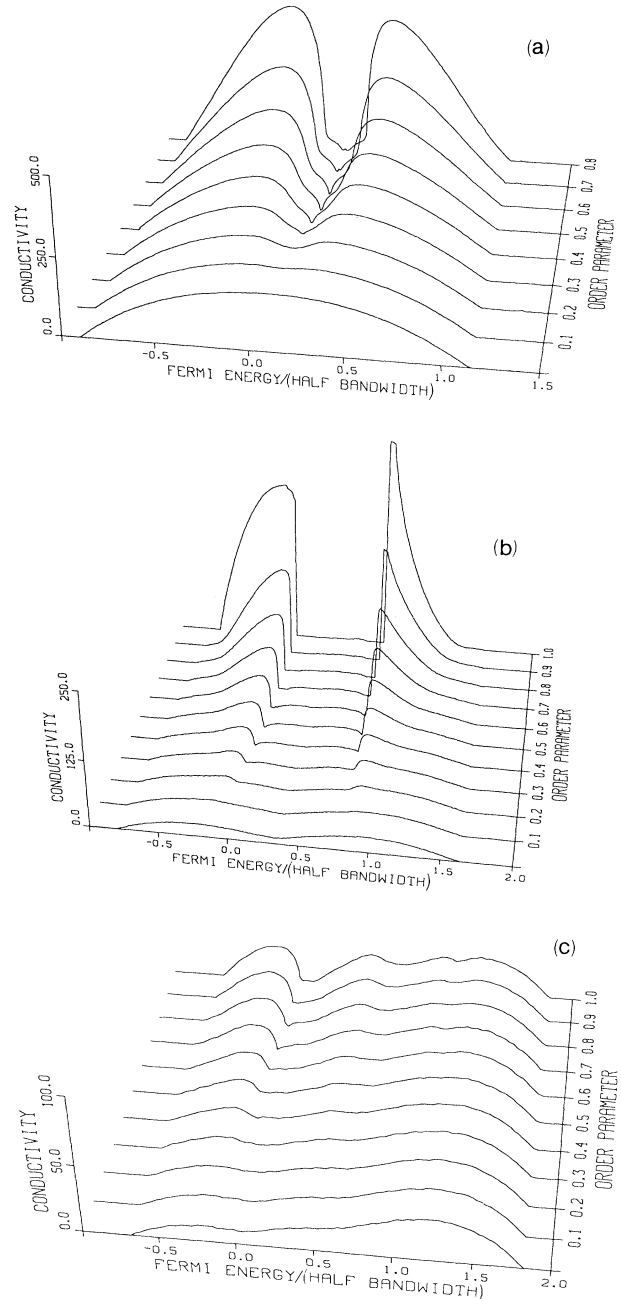


FIG. 4. Conductivity as a function of Fermi energy and ordering with (a) $X_C=0.005$, $X_B=0.48$, $\epsilon_B=0.25$; (b) $X_C=0.05$, $X_B=0.49$, $\epsilon_B=0.75$; (c) $X_C=0.50$, $X_B=0.25$, $\epsilon_B=0.50$.

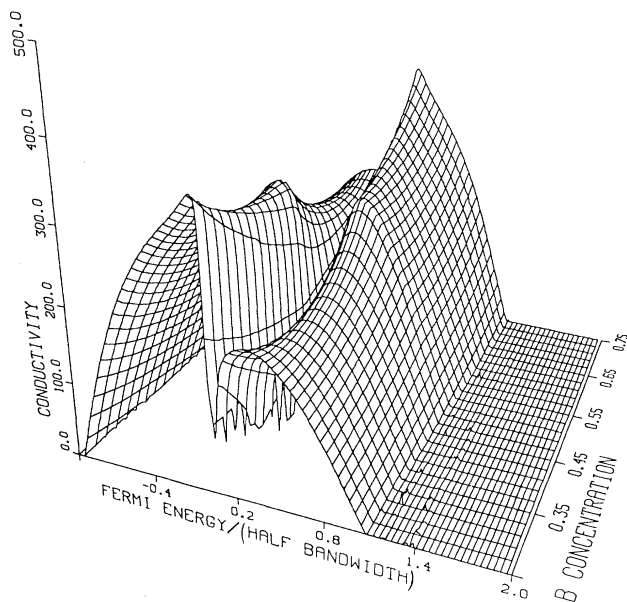


FIG. 5. Conductivity as a function of Fermi energy and B -atom concentration. $\epsilon_B = 0.25$; $\eta = 0.60$.

due to the still present A and B atoms on the “wrong” lattice (we are not at perfect order). These structural features vanish at perfect order in the binary case and are expected to do so here as evidenced by a diminishing height as order is increased. What remains unchanged, however, is the larger right-hand band which can only be attributed to the C atom. Figure 3(b) is a similar plot as before, but now with a B atom energy at 0.75 and order parameter $\eta = 0.95$. The smaller A - and B -atom band structures in the valley center have coalesced in this case and, as before, are expected to disappear altogether at perfect order. The far right band hump is a phenomenon of the C atom.

The surface plots in Figs. 2 and 5 are designed to accentuate what happens to the DOS and conductivity as the B -atom concentration is varied while fixing the value of the order parameter (in this case at 0.6). The C -atom concentration is 0.005 (i.e., near binary) and the B -atom energy is 0.25. The main feature to notice is the variation of the peak as one goes from low to high values of X_B . In particular, at low X_B , the peak is sharp and pronounced on the A -atom energy side while the other side of the valley shows a more rounded form. As one moves to equal concentrations of A and B atoms (i.e., $X_A = X_B$), two peaks are seen on both sides of the valley. Finally, as one moves on toward higher values of X_B , the peak shifts to the B -atom energy side of the valley while the graph becomes more rounded on the other side.

VII. CONCLUSIONS

In this paper we have investigated a ternary alloy model by adding a completely random third atom on a bipartite lattice of an order-disorder binary alloy. Calculation of the temperature dependence of the long-range ordering parameter using moments of the ternary alloy density of states, shows that the order-disorder phase transition is second order (no discontinuous change in entropy) in agreement with the statistical thermodynamic approximation of Bragg and Williams. It is not surprising, as noted in the binary alloy considerations of Ref. 12, that the quasicheical and band methods reach a common result since they are both molecular field theories.

The density of states and the dc electrical conductivity of the ternary alloy have been expressed, in the framework of a generalized coherent-potential approximation, as a function of energy for various concentrations and scattering strengths of the constituents, over the domain of the long-range-ordering parameter. Numerical results show, for both of these quantities, that an increase in the concentration of the third atom generally diminishes the influence of long-range ordering on the formation of the diatomic crystal. It is of interest to note that this behavior is not only seen in the main structural elements of the density of states and conductivity, but also in impurity subbands characteristic of the ternary alloy. The dependence of the conductivity on the density of states at the Fermi energy is revealed in the obvious correlation between corresponding plots of these quantities, over the range of the ordering parameter. Since the electron concentration has a direct bearing on the Fermi energy, we may also view this similarity in terms of increasing or decreasing the number of electrons per atom. Thus, for particular values of the electron concentration, the conductivity of the ternary alloy becomes larger (and in some cases infinite) as the order parameter (temperature) increases (decreases) while for other values it decreases under the same conditions. These trends in the conductivity are weakened (and in some cases washed out) by the disorder of the third atom.

Although this model does not purport to be representative of any particular material, it may be that its properties reflect some features of a real system.

ACKNOWLEDGMENTS

The authors would like to thank the University of Vermont Academic Computing Center for use of the facilities and, in particular, to two members for their special assistance. We thank Steve Cavrak and Wesley Wright for their help with the IMSL library, the graphics routines, and numerical algorithms in general.

¹P. Soven, Phys. Rev. **156**, 809 (1967).

²D. W. Taylor, Phys. Rev. **156**, 1017 (1967); Y. Onodera and Y. Toyozawa, J. Phys. Soc. Jpn. **24**, 341 (1968). For an excellent review of the CPA and its applications, see J. S. Faulkner,

Prog. Mat. Sci. **27**, 1 (1982).

³P. Soven, Phys. Rev. B **2**, 4715 (1970); H. Shiba, Prog. Theor. Phys. **16**, 77 (1971); B. L. Gyorffy, Phys. Rev. B **5**, 2382 (1972).

- ⁴W. H. Butler and G. M. Stocks, *Phys. Rev. B* **29**, 4217 (1984); H. Winter and G. M. Stocks, *ibid.* **27**, 882 (1983); G. M. Stocks and W. H. Butler, *Phys. Rev. Lett.* **48**, 55 (1982).
- ⁵W. H. Butler, *Phys. Rev. B* **31**, 3260 (1985).
- ⁶G. Vignale and W. Hanke, *Z. Phys. B* **69**, 193 (1987); G. Vignale, W. Hanke, and A. A. Maradudin, *ibid.* **69**, 209 (1987).
- ⁷D. Joubert and J. C. Inkson, *J. Phys. C* **1**, 1077 (1989).
- ⁸E-Ni Foo and H. Amar, *Phys. Rev. Lett.* **25**, 1748 (1970).
- ⁹M. Plischke and D. Mattis, *Phys. Rev. B* **7**, 2430 (1973); *Phys. Rev. Lett.* **27**, 42 (1971).
- ¹⁰A. Paja, *J. Phys. C* **9**, 1445 (1976).
- ¹¹S. M. Borodachev, V. A. Volkov, and S. I. Masharov, *Fiz. Metal. Metalloved.* **42**, 1147 (1976).
- ¹²J. Kudrnovský and B. Velický, *Czech. J. Phys.* **27**, 71 (1977).
- ¹³L. M. Scarfone, *Phys. Rev. B* **7**, 4435 (1973); L. M. Scarfone and J. D. Chlipala, *ibid.* **11**, 4960 (1975).
- ¹⁴K. I. Wysokinski and M. Pilat, *J. Phys. C* **9**, 4271 (1976).
- ¹⁵For a preliminary report of this work, see W. Karstens and L. M. Scarfone, *Bull. Am. Phys. Soc.* **35**, 100 (1990).
- ¹⁶W. L. Bragg and E. J. Williams, *Proc. R. Soc. London, Ser. A* **145**, 699 (1934).
- ¹⁷F. J. Brouers, J. Giner, and J. Van der Rest, *J. Phys. F* **4**, 214 (1974).
- ¹⁸J. Hubbard, *Proc. R. Soc. London, Ser. A* **276**, 238 (1963); **277**, 237 (1964); **281**, 401 (1964).
- ¹⁹B. Velický, S. Kirkpatrick, and H. Ehrenreich, *Phys. Rev.* **175**, 747 (1968).
- ²⁰B. Velický, *Phys. Rev.* **184**, 614 (1969).
- ²¹D. A. Greenwood, *Proc. Phys. Soc. London, Sec. A* **71**, 585 (1958).
- ²²R. E. Peierls, *Quantum Theory of Solids* (Oxford, New York, 1955).
- ²³R. Kubo, *J. Phys. Soc. Jpn.* **8**, 20 (1957).
- ²⁴E. Verboven, *Physica* **36**, 1091 (1960).
- ²⁵F. Brouers and A. V. Vedyayev, *J. Phys. F* **3**, 127 (1973).
- ²⁶H. Jones, *The Theory of Brillouin Zones and Electronic States in Crystals* (North-Holland, Amsterdam, 1962).